https://doi.org/10.61092/iaea.8t4w-essq

INDC(NDS)- 0808
Distr. AI+MN+NM

International Atomic Energy Agency

INDC International Nuclear Data Committee

Scission Neutrons from Thermal Neutron induced Fission of ^{239}Pu and Spontaneous Fission of ^{252}Cf

A.S. Vorobyev, O.A. Shcherbakov
Petersburg Nuclear Physics Institute of National Research Center
“Kurchatov Institute”, Gatchina, Russia

February 2020

IAEA Nuclear Data Section
Vienna International Centre, P.O. Box 100, 1400 Vienna, Austria

Selected INDC documents may be downloaded in electronic form
from http://nds.iaea.org/publications
or sent as an e-mail attachment.
Requests for hardcopy or e-mail transmittal should be directed to
NDS.Contact-Point@iaea.org
or to:
Nuclear Data Section
International Atomic Energy Agency
Vienna International Centre
PO Box 100
1400 Vienna
Austria

Printed by the IAEA in Austria

February 2020

INDC(NDS)- 0808
Distr. AI+MN+NM

Scission neutrons from thermal neutron induced fission of ^{239}Pu and spontaneous fission of ^{252}Cf

A.S. Vorobyev, O.A. Shcherbakov
Petersburg Nuclear Physics Institute of National Research Center
"Kurchatov Institute", Gatchina, Russia

ABSTRACT

The properties of "scission" neutrons from thermal-neutron induced fission of ^{239}Pu(n_{th},f) and spontaneous fission of ^{252}Cf(sf) were obtained by comparing experimental angular and energy distributions of the prompt fission neutrons measured recently at PNPI with model distributions calculated under the assumption that all prompt fission neutrons are emitted from fully accelerated fragments.

February 2020

Contents

Introduction

Up to now many theoretical and experimental works were performed to investigate the low energy nuclear fission. A special attention was given to the details of the prompt fission neutron (PFN) emission: spectra and multiplicities, their dependence on fission fragment (FF) characteristics and all possible correlations between reaction products. These data are used widely for the construction of nuclear reactors and applied for the development of non-destructive methods of nuclear safety and for the control of non-proliferation of nuclear materials. Despite considerable progress achieved in description of the properties of prompt fission neutrons (PFNs) [1–4], some discrepancies still exist between the experimental data and results of theoretical calculations. The observed differences are related to both the limitations of theoretical models used to describe the properties of prompt fission neutrons and the absence of necessary experimental data.

Since for theoretical descriptions it is usually assumed that PFNs are emitted from the fission fragments fully accelerated in the mutual Coulomb field, a special attention deserves the question of the existence of scission neutrons emitted from fissioning nucleus during its evolution from equilibrium deformation to the scission point. The search for scission neutrons and investigations of their properties are complicated by impossibility of discriminating in an experiment between these neutrons and neutrons emitted from the fully accelerated fission fragments. These investigations can only be conducted by comparing measured distributions of the PFNs and model calculations performed by assuming that all PFNs are emitted from fully accelerated fragments. In this case, it can be found the yield of neutrons whose emission mechanism differs from evaporation of neutrons from fully accelerated fragments (for example, emission of neutrons before or at the time of scission of a fissioning nucleus or in the process of acceleration of produced fission fragments), such neutrons are called as “scission” neutrons. A final conclusion about validity of any mechanism of such neutron emission can be done only after detailed comparison of predictions made in the framework of different theoretical models with the dependences reliably observed in the experiment.

Experimental studies dedicated to search for “scission” neutrons are limited to spontaneous fission of ^{252}Cf and thermal neutron-induced fission of ^{235}U. In particular, for the most studied case of spontaneous fission of ^{252}Cf(s.f), estimates of the contribution of “scission” neutrons obtained from the analysis of independent experimental data range from 1 to 20% of the total number of neutrons per fission event (Table 1) [5–22]. For thermal neutron-induced fission of ^{239}Pu these investigations are limited to works shown in Table 2 [8, 23-26]. The yield of “scission” neutrons obtained in these works varies from 4 to 30% of the total PFN number per fission event. It can be concluded from Tables 1-2 that the yield of “scission” neutrons is the less, the more sophisticated becomes an experimental technique and the more detailed becomes an analysis of all possible systematic effects.

It should be also noted that the uncertainties of the input parameters used in the model calculation performed under the assumption that all PFNs are emitted from fully accelerated fission fragments leads to the uncertainties of the yield of “scission” neutrons derived from experimental data. In order to exclude these uncertainties, it is necessary to make a comparison of the PFN distributions obtained in the different experiments using the same model and input parameters. But in most of the works mentioned above only the final conclusions are given without presenting all used input parameters and measured data in digital format. There are only two reported sets of data [5, 12] for ^{252}Cf(s.f) and one [26] for ^{239}Pu(n_{th},f) that can be used for joint analysis.

In the present report are given the results of an analysis of the PFN angular and energy distributions from thermal- neutron induced fission ^{239}Pu(n_{th},f) and spontaneous fission ^{252}Cf(s.f) measured recently in NRC KI - PNPI. The comparison of the measured PFN distributions with model ones calculated under the assumption that all PFNs are emitted from fully accelerated fragments is performed. To obtain model distributions, it is assumed to use the spectra of PFNs measured at small angles relative to the preferential direction of movement of light and heavy fragments because it is expected that just for these angles the contribution of non-primary mechanism is minimal, while a contribution of neutrons emitted by complementary fragment can be taken into account correctly It is also very important that in this approach it is possible to obtain the model distributions practically unlimited in low-energy range. In a course of these calculations, it was used a method free of any assumptions about the PFN properties [18, 27].

Table 1. Main results of the investigations of neutron emission mechanism for $^{252}Cf(sf)$.

Authors, References, Experimental Set-up	Yield of "scission" neutrons	Average energy of "scission" neutrons	Anisotropy of PFN emission in the center-of-mass system of fission fragment, A_2
Investigation of (n,f)-angular correlation			
H R. Bowman *et al* [5, 6] (1962). Two plastic scint. for FFs spectroscopy (TOF 100cm);Two neutron detectors (plastic scint.) were used, TOF(100cm). One of them was placed at 11.25° relative to FFs direction. The position of the second detector was varied from 22.5° to 90° in step 11.25°.	10%	2.6 MeV	0.016 ± 0.012
V.M. Piksaikin *et al* [7] (1977). Two Si-surface barrier detectors for FFs spectroscopy; Single-crystal (stilbene) proton-recoil spectrometer was placed interchangeably at 8.7° and 90° relative to FFs direction, n/γ pulse shape discrimination.	20%	1.52 MeV	Not investigated
Yu.S. Zamyatnin *et al* [8] (1979). IC with collimator used for FFs spectroscopy; One neutron detector (plastic scint.) was placed interchangeably at 0° and 90° relative to FFs direction, TOF (40cm).	15 ± 8%	---	Not investigated
P. Riehs [9] (1981). Two Si-surface barrier detectors for FFs spectroscopy; Two neutron detectors (NE213) were placed at 0° and 90° relative to FFs direction, n/γ pulse shape discrimination, TOF(75cm).	5.9 ± 1.3 % (13.2 ± 3.1%)	2.0 MeV	Not investigated
D. Ward *et al* [10] (1983). Three Si-surface barrier detectors to set direction of FFs (0°, 45° and 90°) relative to axis of neutron detector (NE213), n/γ pulse shape discrimination, TOF(34cm)	10 ± 5%	---	Not investigated
E.A. Seregina *et al* [11, 12] (1985). Six Si-surface barrier detectors to set direction of FFs (from 0° to 90° in interval 10°) relative to axis of neutron detector (Single-crystal stilbene proton-recoil spectrometer), n/γ pulse shape discrimination.	10.6 ± 2.1 %	1.5 ± 0.3 MeV	0.07
H. Marten e*t al* [13] (1991). Two parallel-plate avalanche counters for selection of FFs group; Two neutron detectors NE912(6-Li glass) and NE213, TOF(35, 160cm	< 5%	---	0.06
O.I. Batenkov *et al* [14] (1989). Micro channel plates used for FFs spectroscopy (TOF with base 9 cm); Two neutron detectors (stilbene) arranged collinearly were used, n/γ pulse shape discrimination, TOF (37.5, 75, 150cm).	2 - 3 %	---	0.04

Table 1. Main results of the investigations of neutron emission mechanism for $^{252}Cf(sf)$ (continued).

Authors, References, Experimental Set-up	Yield of "scission" neutrons	Average energy of "scission" neutrons	Anisotropy of PFN emission in the center-of-mass system of fission fragment, A_2
Investigation of (n,f)-angular correlation			
H.-H. Knitter *et al* [15, 16] (1992). IC used for FFs spectroscopy and measuring FF angle; One neutron detector (NE213), n/γ pulse shape discrimination, TOF(50 cm).	1.1 ± 0.3 %	0.4 MeV	0.01 ± 0.02
Yu.D. Kamarzhnov *et al* [17] (1998). Two Si-surface barrier for FFs spectroscopy; Two neutron detectors (NE213) were placed at 0° and 90° relative to FFs direction, n/γ pulse shape discrimination, TOF(75cm).	2.5 ± 1.0 %	---	Not investigated
A.S. Vorobyev *et al* [18] (2010). 16 MWPC for FFs spectroscopy (TOF with base 14cm); Two stilbene neutron detectors were used, n/γ pulse shape discrimination, TOF (~50cm). The neutron spectra measurements were done simultaneously for angles ranging from 0° to 180° in interval 18° relative to the light FFs direction.	≤ 5%	---	0.04
Investigation of (n,n)-angular correlation			
J.S. Pringle and F.D. Brooks [19] (1975). Two neutron detectors (NE213), n/γ pulse shape discrimination, TOF (30, 40 and 50cm).	< 10 %	---	Not investigated
A.M. Gagarski *et al* [20] (2008). Two stilbene neutron detectors, n/γ pulse shape discrimination, TOF (40-70 cm). V.E. Sokolov *et al* [21] (2010) reanalysis of [20].	10 - 11 % 8 ± 3%	1.6 MeV 2.0 ± 0.2 MeV	Weakly sensitive
Compilation of (n,f) data from refs [5], [12] *and* [15]			
N.V.Kornilov *et al* [22] (2001).	~ 10%	Two components with average energy 0.9 MeV and 3.0 MeV.	Not investigated

Table 2. Main results of the investigations of neutron emission mechanism for ^{239}Pu(nth,f).

Authors, References, Experimental Set-up	Yield of “scission” neutrons	Average energy of “scission” neutrons	Anisotropy of PFN emission in the center-of-mass system of fission fragment, A_2
Investigation of (n,f)-angular correlation			
J.S. Fraser *et al* [23] (1965). Two plastic scint. for FFs spectroscopy (TOF with the base of 125cm and 99cm). Four neutron detectors (plastic scint.) were used, TOF (106cm). The neutron spectra measurements have been done simultaneously at 10°, 25°, 45° and 80° relative to FFs direction.	30%	~ 2 MeV	“… all results are consistent with A = 0.”
Yu.S. Zamyatnin *et al* [8] (1979). IC with collimator used for FFs spectroscopy; One neutron detector (plastic scint.) was placed interchangeably at 0° and 90° relative to FFs direction, TOF (40cm).	20 ± 12 %	---	Not investigated
A.S. Vorobyev *et al* [24] (2018). 8 MWPC for FFs separation (TOF with base 14cm); Two stilbene neutron detectors were used, n/γ pulse shape discrimination, TOF (~50cm). The neutron spectra measurements were done simultaneously for angles ranging from 0° to 180° in interval 18° relative to the light FFs direction.	4.5 ± 0.9%	1.6 ± 0.2 MeV	0.04 ± 0.2
Investigation of (n,n)-angular correlation			
V.E. Sokolov *et al* [25] (2010). Two stilbene neutron detectors, n/γ pulse shape discrimination. I.S. Guseva *et al* [26] (2018) reanalysis of [25].	14 ± 3% 4.0 ± 1.5%	1.8 ± 0.2 MeV 1.8 ± 0.2 MeV	Weakly sensitive

1. Description of the experimental set-up

The experiments have been done at the radial neutron channel N1 of the research reactor WWR-M (PNPI, Gatchina). The detailed description of measurement technique and data processing has been given elsewhere [27-29]. At present, the commonly accepted international standard for measuring PFN spectra is established by the integral PFN spectrum of spontaneous ^{252}Cf fission [30]. For this reason, measurements of the angular and energy distributions of PFNs from thermal neutron-induced fission of ^{239}Pu were performed in comparison with the spectra of spontaneous ^{252}Cf fission under identical experimental conditions using a setup that was previously used for analogous investigation [18]. The spectra of PFN were measured simultaneously for 11 angles between the direction of emission of a neutron and the direction of motion of a light fragment in the range of 0°–180° with a step of 18°. Taking into account the real geometry and angular resolution of experimental set-up, these angles were 8.8°, 19.9°, 36.8°, 54.5°, 72.2°, 90°, 107.8°, 125.5°, 143.2°, 160.1°, and 171.2°. The energies of PFNs and velocities of fission fragments were determined using the time-of-flight (TOF) technique. The measurements were carried out in repeated cycles. Each cycle included sequential measurements of the angular and energy distributions of PFNs from ^{239}Pu(n, f) and ^{252}Cf(sf) reactions. The ^{252}Cf target was located in the reaction chamber at the same position as the ^{239}Pu target.

The PFNs were detected by two neutron scintillation detectors (stilbene crystals ∅50 mm × h50 mm and ∅40 mm × h60 mm mounted on the Hamamatsu-R6091 phototubes) positioned at an 90° angle between their respective axes at a distance of about 50cm from the fissile target. Both neutron detectors were shielded by a cylindrical shield made of a 30mm thick layer of lead and a 40mm thick layer of polyethylene. The neutron registration threshold was ~200 keV. A double-discrimination method (pulse shape and time-of-flight) was used to separate the events produced by neutrons and γ-quanta. The total time uncertainty of timing of signals of neutron detectors, which is determined as the FWHM of peak of γ-ray photon–fragment coincidences, was 1.0–1.2 ns.

The multi-wire proportional detectors (MWPD) were used to detect fission events and to determine directions of motion of fission fragments. The start MWPD located at a distance of 7 mm from the fissile target and parallel to the target plane was mounted together with the target holder-ring on a special frame located in the center of the reaction chamber filled with isobutene (~ 4 Torr) in such a way that all hardware parts were well out of the path of the neutron beam. The stop MWPDs were placed in the form of two arcs of eight detectors in the reaction chamber on a circle at a distance of 140 mm from the center of the chamber. The neutron beam was directed along the chamber axis.

2. Model

2.1. General

The yield of “scission” neutrons is estimated by comparing the measured distributions of PFNs with model calculations under the assumption that all PFNs are emitted from fully accelerated fragments. Within this model, the spectrum of PFNs in the center-of-mass system of a fission fragment with known mass and kinetic energy completely determines the spectrum of PFNs in the laboratory system. As it was shown early (for example, in ref. [31-33]), to construct model distributions of PFNs such as the angular and energy distributions $N(E, \theta)$ and total spectrum $\Phi(E)$, it is possible to use the approximation of two fragments according to which PFNs are emitted in the process of fission from two (light and heavy) fully accelerated fragments with fixed average masses and energies taken from literature (for instance, see Appendix 1-2). In this approach, the following equations are used:

$$\varepsilon = \overline{E}_{f,K} + E - 2 \cdot \cos(\theta)\sqrt{E\overline{E}_{f,K}} \tag{1}$$

$$\sqrt{\varepsilon}\cos(\theta_c) = \sqrt{E} \cdot \cos(\theta) - \sqrt{\overline{E}_{f,K}} \tag{2}$$

$$\overline{E}_{f,K} = \left\langle \frac{\nu_K(m_f, TKE) \cdot TKE}{\overline{\nu}_K} \cdot \left(\frac{1}{m_K} - \frac{1}{A}\right) \right\rangle \approx F_K \cdot \overline{TKE} \cdot \left(\frac{1}{\overline{m}_K} - \frac{1}{A}\right) \tag{3}$$

Here, $K = L$ or H is the index indicating the light or heavy fragment, respectively; $F_K = 0.94$–0.97 is the coefficient reflecting the dependence of the yield of the PFNs on the characteristics of the fragment [34]; $\overline{\nu}_K$ is the average number of neutrons per fission event for the light or heavy fragment; $\nu_K(m_f, TKE)$ is the average number of emitted neutrons as a function of the fragment characteristics; $\overline{TKE}$ is the average total kinetic energy of fission fragments; $\overline{m}_K$ is the average mass of the light or heavy fragment; $\overline{E}_{f,K}$ is the average energy per nucleon, which are 0.949 ± 0.007 MeV and 0.995 ± 0.007 MeV for the light ($K = L$) fragments and 0.540 ± 0.004 MeV and 0.511 ± 0.004 MeV for heavy ($K = H$) fragments for ^{252}Cf(sf) and ^{239}Pu(n,f), respectively.

Then, the number of neutrons emitted from light or heavy fragments within unit energy interval per unit solid angle with the energy E at the angle θ with respect to the direction of fragment motion in the laboratory system, $n_K(E, \theta)$, is related to the analogous number of neutrons emitted with the energy ε at the angle θ_c with respect to the direction of fragment motion in the center-of-mass system of the fragment, $\psi_K(\varepsilon, \theta_c)$, by means of the following formulas:

$$n_K(E,\theta) = \sqrt{\frac{E}{\varepsilon}} \cdot \psi_K(\varepsilon,\theta_c) = \sqrt{\frac{E}{\varepsilon}} \cdot \psi_K(\varepsilon) \cdot \varphi(\varepsilon,\theta_c) \tag{4}$$

$$\varphi(\varepsilon,\theta_c) = 1 + A_2 \cdot \varepsilon \cdot P_2(\cos\theta_c) \tag{5}$$

where function $\varphi(\varepsilon, \theta_c)$ is the angular distribution of neutrons in the center-of-mass system, $P_2(\cos\theta_c)$ is the second-order Legendre polynomial, A_2 is the anisotropy parameter of the angular distribution of PFNs in the center-of-mass system of the fission fragment due to a large angular momenta of the fragments (~ 7ħ on average) [35-37].

The number of neutrons $N(E, \Omega)$ with energy E registered at angle Ω relative to the light fragment's direction in the laboratory system can be represented as the sum of contributions from the light $n_L(E, \Omega)$ and heavy fragments $n_H(E, \Omega)$:

$$N(E,\Omega) = n_L(E,\Omega) + n_H(E,\Omega)\ , \tag{6}$$

$$n_L(E,\Omega) = n_L(E,\theta + \Delta_1) \qquad \text{and} \qquad n_H(E,\Omega) = n_H(E,180 - \theta + \Delta_2)\,,$$

where Δ_1 and Δ_2 are the terms due to the neutron recoil effect. In a case of thermal neutron induced fission, the deviations of fragment's directions of motion from co-linearity due to neutron recoil effect does not exceed 2° on average [38, 39], the terms Δ_1 and Δ_2 are usually taken equal to zero. In this work, this correction was calculated (see Fig. 1) using the equation given in [39]. The integral spectrum $\Phi(E)$ of PFNs in the laboratory system is defined as follows:

$$\Phi(E) = 2\pi \cdot \int_0^{\pi} N(E,\Omega)\sin(\Omega)d\Omega \tag{7}$$

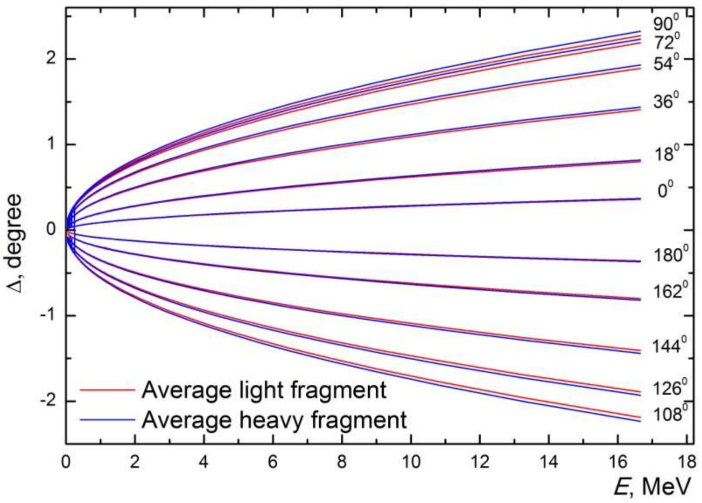

Fig. 1. *Energy dependence of the correction due to neutron recoil for fixed angles θ given in the right part of the figure.*

According to the structure of Eq. (4), the spectra of PFNs in the center-of-mass system of the fission fragment, $\psi_K(\varepsilon)$, can be obtained from the spectra of the PFNs measured at different angles with respect to the direction of fragment motion, $n_K(E, \theta)$. In this case, an individual spectrum of PFNs in the center-of-mass system of the fragment, $\psi^{\theta}_K(\varepsilon)$, is obtained for each given direction θ:

$$\psi_K^{\theta}(\varepsilon) = \sqrt{\frac{\varepsilon}{E}} \cdot \frac{n_K(E,\theta)}{1 + A_2(\varepsilon) \cdot P_2(\cos\theta_c)} \tag{8}$$

Assuming that the hypothesis of neutron emission from fully accelerated fission fragments is valid, the spectra of neutrons in the center-of-mass system of fission fragment, $\psi^{\theta}_K(\varepsilon)$, determined by Eq. (8) will be identical for all selected directions θ within the achieved accuracy of experimental data. Therefore, deviation of the measured angular and energy distributions of neutrons from the respective distributions calculated by Eqs. (4)–(7) using the spectra of neutrons in the center-of-mass system of fission fragment, $\psi^{\theta}_K(\varepsilon)$, will characterize the accuracy of the adopted model.

The spectra of PFNs in the center-of-mass system of light and heavy fission fragments, $\psi^{\theta}_K(\varepsilon)$, were obtained in the approximation of two fragments with the use of the spectra of PFNs, $N(E, \Omega)$, measured at small angles with respect to the direction of motion of the light ($\Omega < 40°$) and heavy ($\Omega > 140°$) fragments. In this case, we used only collected events for which $0 \leq \theta \leq 90°$ (prompt fission neutrons are emitted into the forward hemisphere with respect to the direction of motion of the fragment):

$$\sqrt{E} \cdot \cos(\theta) \geq \sqrt{\bar{E}_{f,K}} \quad . \tag{9}$$

Thus, the spectrum of PFNs in the center-of-mass system of fragments that is almost unlimited in the region of low energies can be obtained and, therefore, the uncertainty of model calculations caused by uncertainties in the shape of the spectrum and in the number of prompt fission neutrons emitted from light and heavy fragments can be minimized.

It should be noted that the spectrum of PFNs measured for each given direction θ includes a fraction of neutrons from the complementary fragment. Consequently, before using the measured spectra of PFNs to determine the spectra of PFNs in the center-of-mass system of the fission fragment, the contribution from the emission of PFN from the complementary fragment should be subtracted from them. The procedure included the following steps.

At the first step, it is assumed that neutrons detected at small angles relative to the light fragment's direction of motion in the laboratory system ($\Omega < 40°$ for light fragments and $\Omega > 140°$ for heavy fragments) are emitted from only the light and heavy fragments, respectively. Then, the neutron spectra measured for selected angles can be used for calculating neutron spectra in the center-of-mass system for the corresponding light and heavy fragments using Eq. (8). At the second step, the contribution of neutrons from the complementary fragment determined in the first step was subtracted from the spectra measured at small angles in the laboratory system. After that, the spectra of the PFNs in the center-of-mass system of the light and heavy fission fragments were recalculated and approximated by the following function with parameters ($\bar{\nu}_K$,ω_K, T_{1K}, T_{2K}) determined by the least squares method:

$$\psi_K(\varepsilon) \cong Fit_K(\varepsilon) = \frac{\bar{\nu}_K}{4\pi} \cdot \left[\varpi_K \cdot \frac{\varepsilon}{T_{1K}{}^2} \cdot \exp\left(-\frac{\varepsilon}{T_{1i}}\right) + (1-\varpi_K) \cdot \frac{2\cdot\sqrt{\varepsilon}}{\sqrt{\pi \cdot T_{2K}{}^3}} \cdot \exp\left(-\frac{\varepsilon}{T_{2K}}\right) \right] \tag{10}$$

Here, $\bar{\nu}_K$ is the average number of neutrons per fission event for a light or heavy fragment ($\bar{\nu}_p = \bar{\nu}_L + \bar{\nu}_H$); ω_K is the weighing function; and T_{1K}, T_{2K} are the corresponding distribution parameters. For the convenient use and simplification of model calculations, function (10) was further used as the spectra of PFNs in the center-of-mass system of light and heavy fragments instead of discrete distributions obtained from experimental data. These basic spectra of neutrons in the center-of-mass system of fragments (for example, in Figs. 2, 3 the spectra obtained for ^{239}Pu(n,f) and ^{252}Cf(sf) are presented, respectively) were used for calculating (with the help of expressions (4)–(7)) the angular and energy distributions of PFNs in the laboratory system, corresponding to the model of neutron emission from fully accelerated fission fragments.

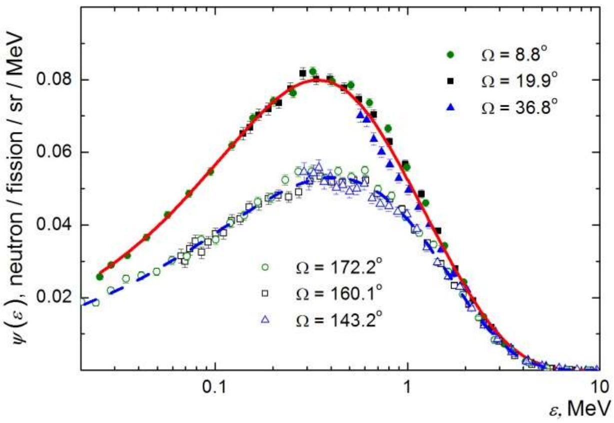

Fig. 2. *The PFN spectra of ^{239}Pu(n, f) in the center-of-mass system of (black symbols) light and (open symbols) heavy fragments, obtained from spectra in the laboratory system in the two-fragment approximation for selected angles Ω between the neutron emission and light fragment escape directions; curves show the approximation according to formula (10).*

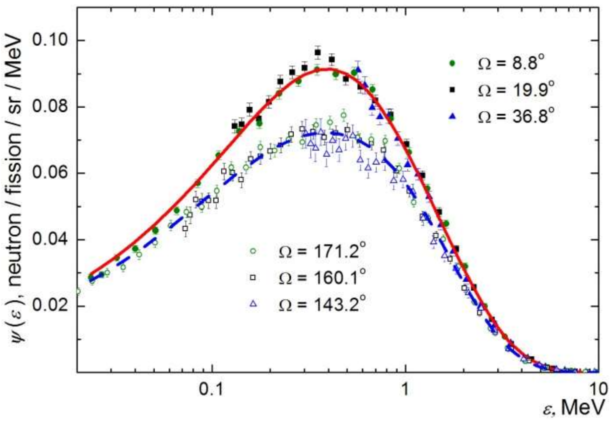

Fig. 3. *The PFN spectra of ^{252}Cf(sf) in the center-of-mass system of (black symbols) light and (open symbols) heavy fragments, obtained from spectra in the laboratory system in the two-fragment approximation for selected angles Ω between the neutron emission and light fragment escape directions; curves show the approximation according to formula (10).*

2.2. Determination of the model parameters

As was mentioned above, the ^{252}Cf is a most studied nucleus and the total spectrum of PFNs from ^{252}Cf(sf) is a high accuracy international standard. For this reason, to optimize the model, which is used to describe the measured angular and energy distributions of PFNs, and to determine its confidence, we compare the PFNs distributions of ^{252}Cf(sf) calculated under different model assumption with the standard spectrum from ref. [30].

The main advantage of the discussed model is that, after the average energy per nucleon is determined, the model includes only one varying parameter A_2 responsible for the anisotropy of the angular distribution of PFNs in the center-of-mass system of the fission fragment from which neutrons are emitted. In this case, the test of confidence of the model is reduced to the determination of the difference between experimental data and model calculations. The analysis of data showed that the best description of the total spectrum of PFNs is achieved simultaneously with the best description of the partial spectra of PFNs [40].

Figure 4 shows the standard total spectrum of PFNs from ^{252}Cf [30] and the model spectrum of PFNs calculated within the above scheme. In order to indicate more clearly the existing differences, the spectra of PFNs are presented as the ratio to the Maxwell distribution $M(T_M, E)$ (T_M = 1.42 MeV):

$$\mu(E) = \frac{\Phi(E)}{\bar{\nu}_p \cdot M(T_M, E)} = \frac{\Phi(E) \cdot \sqrt{\pi \cdot T_M^{\,3}}}{\bar{\nu}_p \cdot 2 \cdot \sqrt{E} \cdot \exp(-E/T_M)} \tag{11}$$

where $M(T_M, E)$ is the Maxwell distribution, T_M is the temperature parameter (average energy of the Maxwell distribution $< E > = 3T_M/2$). The calculation under the assumption that A_2 = 0 (spectra obtained from the spectra measured at angles of 8.8°and 172.1° were used as the reference spectra) is also shown in this figure for comparison. Errors corridor for one of the calculated model total spectra caused by uncertainty in the measured spectra of neutrons, which were used to determine the reference spectra, are also shown. To demonstrate the effect of anisotropy on the shape of the total PFNs spectrum, the total spectra of PFNs calculated under different assumptions on the anisotropy parameter are shown in Fig. 5.

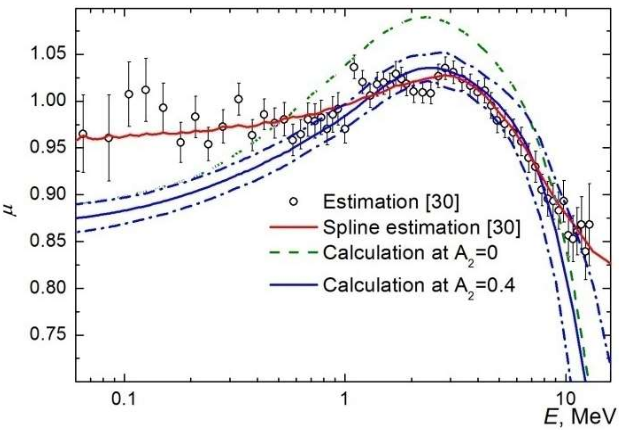

Fig. 4. Ratio of the total PFN spectrum of ^{252}Cf(sf) (normalized to average PFN number per fission) to the Maxwell distribution (T_M = 1.42 MeV): circles and red curve passes through them show the standard spectrum from [30], green dash curve shows the result of calculations at A_2 = 0, and blue curve (uncertainties are limited by blue dash-dot curves) shows the result of calculation at A_2 = 0.04.

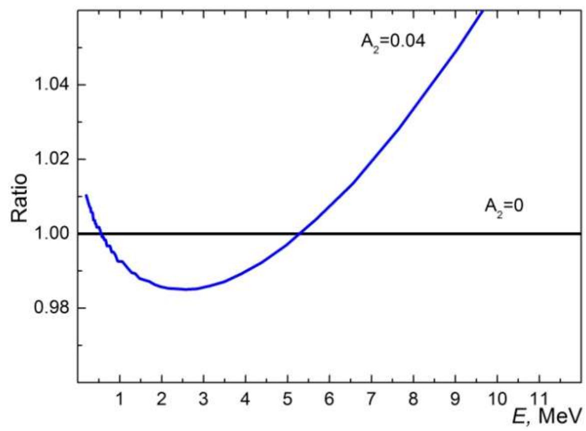

***Fig. 5.** Curves corresponding to A_2 = 0 and A_2 = 0.04 show the ratios of the total spectra of PFNs in the laboratory system obtained in two fragments approximation with the same reference spectra (calculated using PFNs spectra measured for angles Ω < 40° and Ω > 160°) and under different assumptions on the anisotropy parameter A_2.*

Yield of PFNs from ^{252}Cf(sf) versus the angle between the direction of emission of a neutron and the direction of motion of the light fragment in the laboratory system calculated as mentioned above is presented in Fig. 6 in comparison with the data measured at PNPI and from [5]. In order to perform correct comparison, the model calculations and the data obtained in these works were analyzed in the same energy range (0.55–10.3 MeV) for PFNs as the data from [5]. There is only a small difference most clearly seen in Fig. 7, where ratios of the angular distributions of the yield of PFNs that are obtained in [40] to the model distribution are shown.

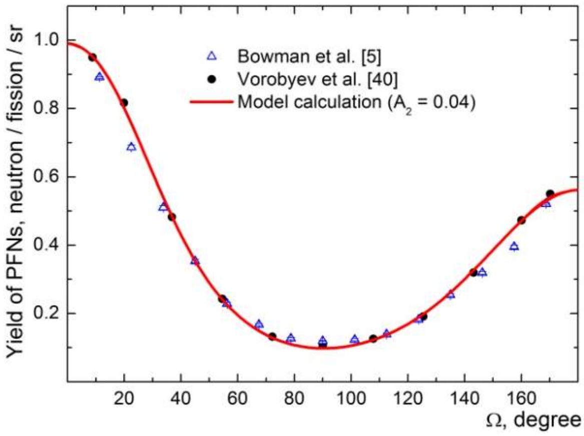

Fig. 6. *Yield of PFNs from $^{252}Cf(sf)$ versus the angle between the direction of emission of a neutron and the direction of motion of the light fragment in the laboratory system.*

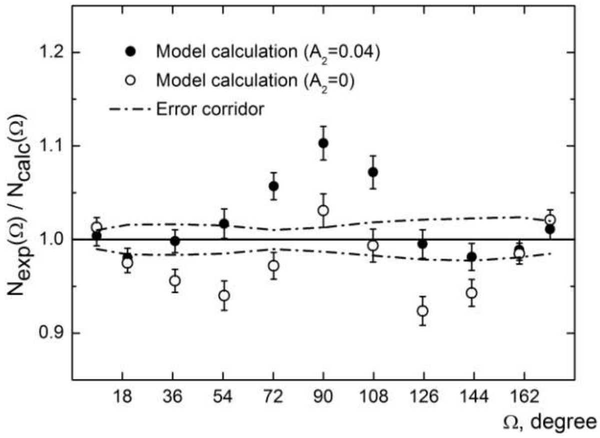

Fig. 7. *Ratio of the measured PFN yield to the neutron yield calculated for A_2=0.04 and A_2=0. The interval of the errors due to uncertainty of the PFN spectra in the fragment center-of-mass system is limited by dotted and dashed curves.*

Since a largest observed relative yield of "scission" neutron is expected for the angles close to 90°, several authors tried to find these neutrons by the investigation of the ratio of the PFNs spectra measured at 0° and 90° relative to the direction of motion of fission fragments. Such a dependence is shown in Fig. 8, 9. Good agreement can be seen between the dependence for model calculation and works [13, 15, and 40], where the spectra of PFNs were determined from the time of flight and the pulse shape separation scheme was used to separate events corresponding to neutrons and γ-ray photons. The pulse shape separation scheme was not applied in [5]. This is possibly an origin of the difference between these data for neutron energies higher than 3 MeV and other data shown in Fig. 9. The ratio of the PFNs spectra obtained using the data from ref. [12] coincides in shape with the results obtained by the time-of-flight method, but a certain difference is observed at neutron energies lower than 2 MeV and the entire dependence is shifted in absolute value. Since corrections were introduced in the response function of the recoil proton spectrometer in the cited work according to the comparison of the measured total spectrum with the standard spectrum of ^{252}Cf, one of the reasons for such difference can be the presence of a disregarded neutron background in the measured amplitude spectra of PFNs. Sources of this background can be, e.g., scattering of neutrons within the solid detection angle, the transmission of the shadow cone, the existence of background of random coincidences, and the possible superposition of events from neutrons and γ-ray photons.

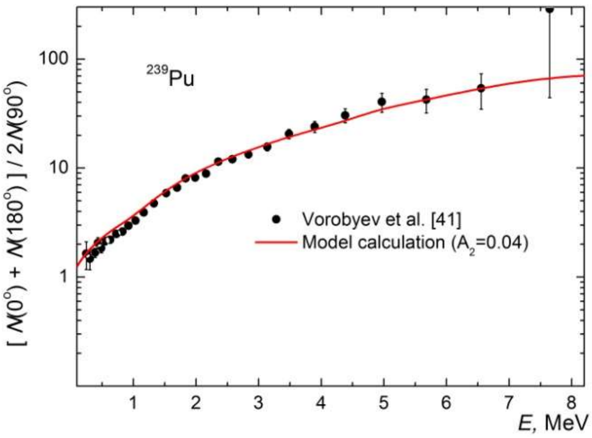

Fig. 8. Energy dependences of the ratio of neutron yields for angles 0° and 90°. Curve is description within the model considering the anisotropy of emission of PFNs in the center-of-mass system of fission fragments, A_2 = 0.04.

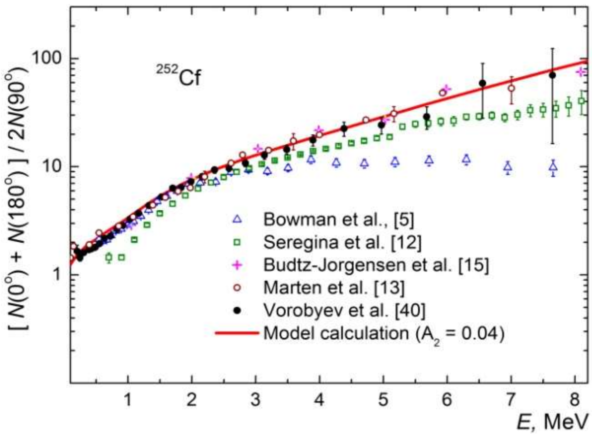

Fig. 9. Energy dependences of the ratio of neutron yields for angles 0° and 90°. Data of the time-of-flight measurements from (●) [40], (+) [15], (○) [13], and (△) [5]. Data from the recoil proton spectrometer shown by squares (green) are taken from [12].

The following features should be emphasized:
first, the description of experimental data is improved if spectra measured for angles Ω < 40° (light fragments) and Ω > 160° (heavy fragments) rather than only spectra for small and large angles of 8.8° and 172.1°, respectively, are used as the reference spectra. This occurs because, first, the statistical accuracy of the initial spectra used to obtain the spectra in the center of-mass system of the fragment is improved and, second, the existing systematic error caused by uncertainty of the standard spectrum of PFNs from ^{252}Cf and by difference in the conditions of measurements of the spectra of PFNs for different angles is partially compensated.
Second, the inclusion of the anisotropy of emission of PFNs in the center-of-mass system of the fission fragment in model calculations also improves the description of experimental data. The best description of experimental data is achieved with $A_2 = 0.04 \pm 0.02$ ($\psi(0°)/\psi(90°) \approx 1.08$). In previous works, the parameter of anisotropy A_2 of the angular distribution of PFNs in the center-of-mass system of ^{252}Cf(sf) fission fragment was also estimated and was 0.04 [14], 0.01±0.02 [15], and 0.04±0.02 [40]. In a more recent investigation [42], it was found that $A_2 = 0.020 \pm 0.003$. Analysis of the integral PFN spectrum of ^{252}Cf in the framework of modified Madland–Nix model [43] also showed the presence of anisotropy for PFN emission in the center-of-mass system of fission fragments.
In this work, the preliminary processing and the determination and introduction of corrections were done in a similar way for ^{239}Pu(n_{th}, *f*) and ^{252}Cf(s.f) as well as for ^{235}U(n_{th}, *f*), ^{233}U(n_{th}, *f*) performed earlier. The parameters of the model used to calculate the angular and energy distributions of PFNs by assuming that they were emitted from the fully accelerated fragments were optimized to produce the best description of all data obtained in PNPI [4].

3. Results

Figures 10 and 11 show the energy spectra of PFNs from ^{239}Pu(n_{th},f) and ^{252}Cf(sf), respectively, measured in the laboratory system in comparison with the results of model calculations performed under the assumption of PFN emission from only the fully accelerated fission fragments. On the whole, the calculated model energy and angular distributions agree rather well with the experimentally obtained distributions. However, there is a surplus of neutron yield for angles close to 90° over model calculation (see Figs. 12, 13).

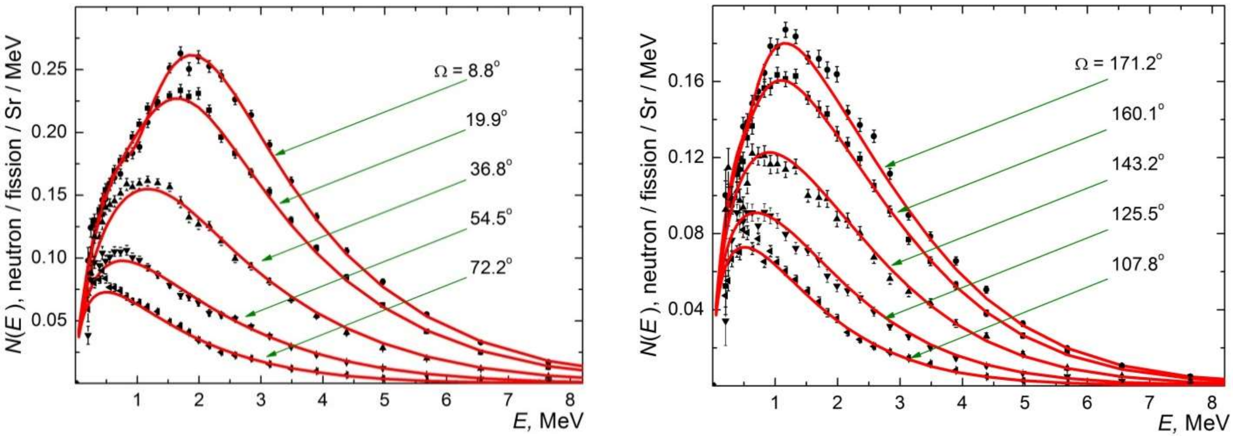

Fig. 10. *Energy spectra of PFNs from* ^{252}*Cf(sf) in the laboratory system for fixed angles of emission of a neutron with respect to the direction of motion of the light fragment indicated near the lines [40]. The indicated errors are statistical. Lines correspond to model calculation (*A_2 *= 0.04)*

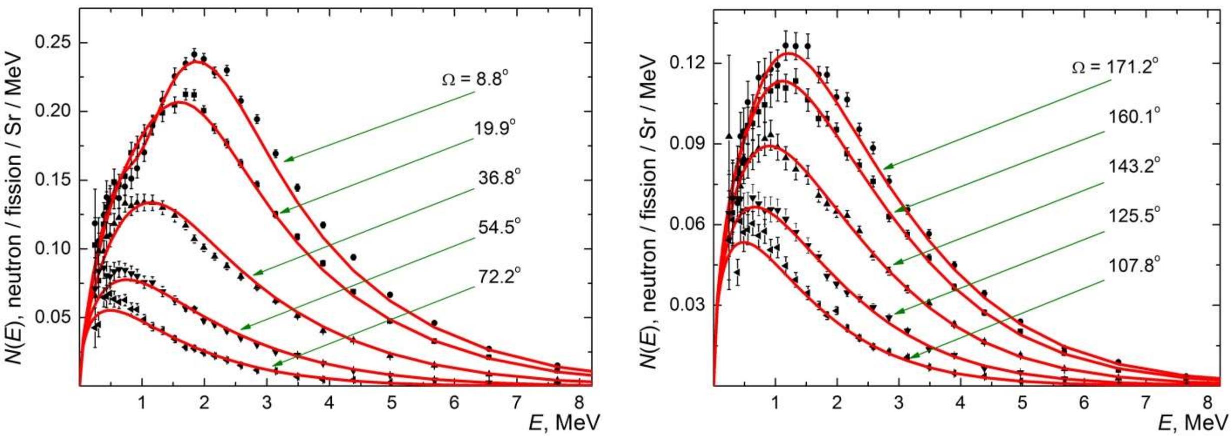

Fig. 11. *Energy spectra of PFNs from* ^{239}*Pu(*n_{th}*,f) in the laboratory system for fixed angles of emission of a neutron with respect to the direction of motion of the light fragment indicated near the lines [41]. The indicated errors are statistical. Lines correspond to model calculation (*A_2 *= 0.04)*

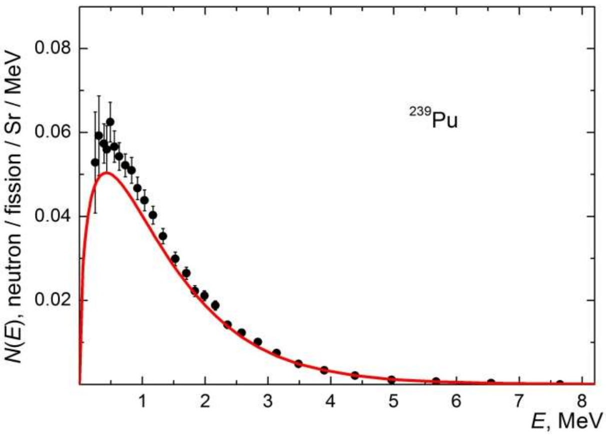

Fig. 12. *Energy spectra of PFNs from* ^{239}*Pu(*n_{th}*, f) measured in the laboratory system at 90° angle relative to the direction of motion of light fragments [41]. Bars indicate statistical errors. Solid curves present the results of model calculations (*A_2 *= 0.04).*

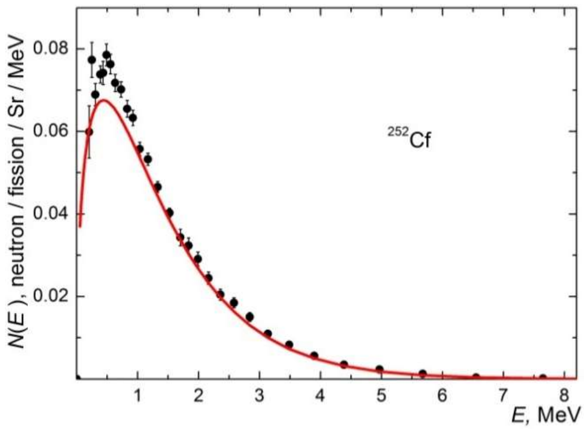

Fig. 13. *Energy spectra of PFNs from* ^{252}*Cf(sf) measured in the laboratory system at 90° angle relative to the direction of motion of light fragments [40]. Bars indicate statistical errors. Solid curves present the results of model calculations (*A_2 *= 0.04).*

The total PFN spectra of ^{252}Cf(sf) and ^{239}Pu(n_{th},f) fission are presented in Figs. 4 and 14, respectively, reveal some differences between the shape of experimental (estimated) PFN spectra and that of the spectrum calculated using the scheme described above (for two-fragment approximation) in the range of PFN energies below 0.6 MeV.

It should be noted that the experimental partial and total spectra of PFNs includes all PFNs emitted during fission, while the calculated spectra only include neutrons emitted from fully accelerated fragments. Therefore, the observed deviation can be treated as evidence of the existence of “scission” neutrons and, hence, their yield can be determined from the difference between experimental and calculated spectra.

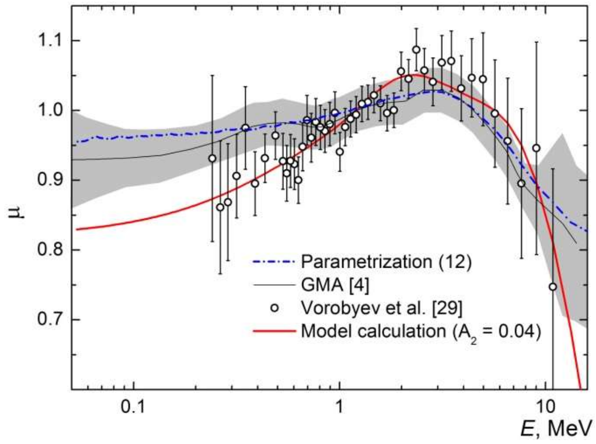

Fig. 14. *Ratio of the total PFN spectrum of* ^{239}*Pu(*n_{th}*,f) (normalized to average PFN number per fission) to Maxwell distribution (*T_M *= 1.38 MeV): circles present data of measurements [29]; (black solid curve) estimated data (GMA [4]) with uncertainty area indicated by gray shade; (dash-dot [blue] curve) parameterization according to (12); (bottom [red] curve) two fragment approximation with anisotropy parameter* A_2 *=0.04.*

In order to exclude the influence of the shape of total PFN energy spectrum on the estimated yield of “scission” neutrons, the measured angular and energy distributions have been additionally corrected for neutron detector efficiency.

This correction factor was defined as the ratio of total PFN spectra of $^{239}Pu(n_{th},f)$ from ref. [29] to the corresponding known total PFN spectra. The reference spectrum was obtained using the following equation:

$$\left(\frac{\Phi(E)}{\bar{\nu}_p}\right)_{Pu} \Bigg/ \left(\frac{\Phi(E)}{\bar{\nu}_p}\right)_{Cf} = \frac{M(1.382, E)}{M(1.42, E)} \tag{12}$$

Since the Maxwell distribution parameter T_M =1.42 MeV was established [30] to provide the best description of experimental total PFN spectrum of ^{252}Cf and the final average energy derived from GMA approximation [4] are 2.073±0.010 MeV (T_M =1.382 MeV) for ^{239}Pu, these parameters were used for obtaining additional corrections. The spline approximation $\Phi(E)$ of the estimated ^{252}Cf fission spectrum reported in [30] was adopted as reference total spectrum of PFNs from ^{252}Cf spontaneous fission for Eq. (12). It is convenient because it enables to make a recalculation later when the numerical data on the evaluated spectra are absent. The reference total PFN spectra of $^{239}Pu(n_{th},f)$ fission calculated using Eq. (12) are presented in Fig. 14 together with the results of estimation (GMA approximation [4]) obtained from published experimental data by generalized least squares method. As can be seen, the relation (12) and model independent estimation based on GMA approximation [4] can be used for determination of the additional corrections.

It was found that for neutron detection angles Ω = 90°, a neutron excess is observed relative to the model calculations: 8.5±3.2% and 7.6±2.8% for ^{239}Pu and ^{252}Cf, respectively. Then, the yield of “scission” neutrons and their spectrum were also determined. As an example, Fig. 15 shows the angular dependence of the yield of “scission” neutron from $^{239}Pu(n_{th},f)$ fission obtained as a difference between yields of PFNs measured and calculated ones in the assumption that all PFNs was emitted from fully accelerated fragments. For comparison, the calculations performed by Carjan et al [44, 45] for $^{235}U(n_{th},f)$ fission in the framework of dynamical scission model under different initial condition are presented together with the yield of “scission” neutrons from $^{235}U(n_{th},f)$ fission obtained by us earlier. The qualitative agreement can be seen which leads to the conclusion that the PFN angular and energy distributions can be described using an assumption that the observed neutron excess is associated with the dynamical effects analogous to those proposed in [44, 45]. In Fig. 16, it is shown the spectrum of ^{239}Pu “scission” neutrons obtained in two different ways. In the first, the desired spectrum was defined as the difference between the measured and model neutron spectra for angles Ω close to 90° (Ω = 72.2°, 90° и 108.8°). In the second, the total spectrum of “scission” neutrons was defined as the difference between the reference total PFNs spectrum and model calculation. To compare the two estimates, the “scission” neutron spectrum obtained in the first way was multiplied by 4π (it was assumed that the distribution of “scission” neutrons in the laboratory system was isotropic). A comparison of the spectra obtained in this manner shows the agreement (within the errors of the experimental data) between the results of estimates performed in different ways.

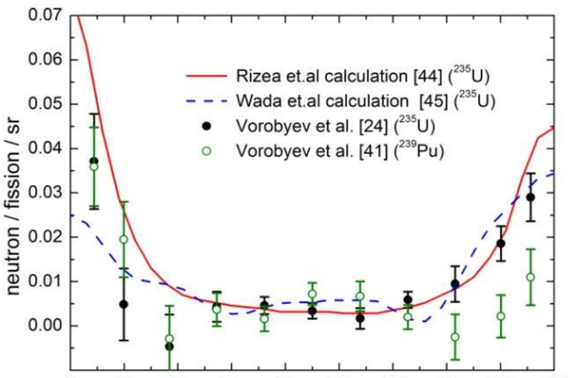

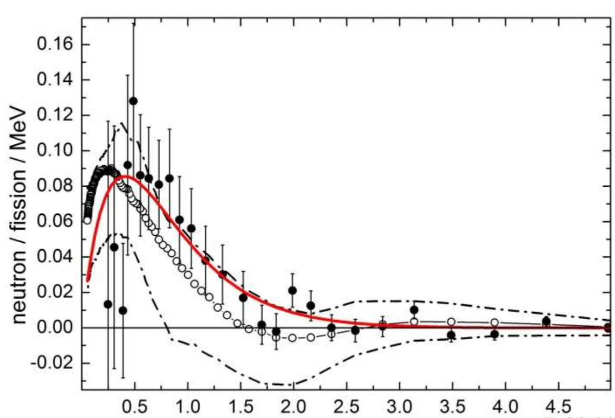

Fig. 15. *Angular dependence of the yield of "scission" neutrons from $^{235}U(n_{th},f)$ fission: (●, ○) the difference between the measured and model yields for the angles Ω, the indicated errors include statistical errors and the uncertainty of model parameters. Solid (red) curve – Rizea et.al calculation [44] performed on the surface of a sphere of radius R=30 fm and for time T further away from the moment of scission $2\cdot10^{-21}$ sec. Dash line Wada et.al calculation [45] – R=50 fm, T = $4\cdot10^{-21}$ sec and the effects of the scattering and re-absorption by the fission fragments on the angular distribution of scission particles were included into calculation.*

Fig. 16. *Spectrum of "scission" neutrons from the $^{239}Pu(n_{th},f)$ fission: (●) the difference between the measured and model neutron spectra for the angles Ω close to 90° (Ω = 72.2°, 90°, 108.8°) multiplied by 4π (first approach), the indicated errors are statistical; (–○–) the difference between the reference total PFN spectrum obtained by means of Eq. (12) and the model calculated total PFN spectrum (second approach). The interval of errors arising from uncertainty of the reference PFN spectrum is limited by the dotted-and-dashed lines. The curve (red) is the approximation by function (13).*

Since the relative contribution from "scission" neutrons should be largest at angles Ω close to 90°, the yield of these neutrons from the fission of the investigated nuclei was estimated using the spectrum obtained in the first way: with least squares approximated by functions (13) and (14):

$$p_s(E) = p_0 \cdot \frac{E}{T_0^{\,2}} \cdot \exp\left(-\frac{E}{T_0}\right), \qquad (13)$$

$$p_s(E) = p_0 \cdot \frac{E}{T_0^{\,2}} \cdot \exp\left(-\frac{E}{T_0}\right) + p_1 \cdot \frac{E}{T_1^{\,2}} \cdot \exp\left(-\frac{E}{T_1}\right). \qquad (14)$$

All parameters p_0, T_0, p_1, T_1 were varied. The results of these approximations are given in Table 3 with the results obtained by us earlier for ^{233}U(n_{th},f) and ^{235}U(n_{th},f).

Table 3. Main characteristics of "scission" neutrons.

	^{233}U(n_{th},f)	^{235}U(n_{th},f)	^{239}Pu(n_{th},f)	^{252}Cf(sf)
Approximation using function (19)				
Yield, %	1.5 ± 0.6	1.8 ± 0.6	3.6 ± 0.5	2.0 ± 0.6
Average energy, MeV	0.53 ± 0.08	0.47 ± 0.05	0.91 ± 0.19	0.58 ± 0.06
Approximation using function (20)				
Yield, %	2.7 ± 0.8	2.6 ± 0.8	4.5 ± 0.9	3.0 ± 0.8
Average energy, MeV	1.7 ± 0.2	1.4 ± 0.2	1.6 ± 0.2	1.5 ± 0.2

The obtained difference spectra (“scission” neutron spectrum) for spontaneous ^{252}Cf fission in comparison with the calculation taking into account non-adiabatic effects in the interaction of the single-particle degrees of freedom with fragment acceleration [46] is shown in Fig. 17. It is seen that the spectrum of “scission” neutrons [46] can be qualitatively described, as well as angular dependence of their yield [44, 45], by assuming that the neutron excess observed in the experiment was due to the dynamic effects in nuclear fission.

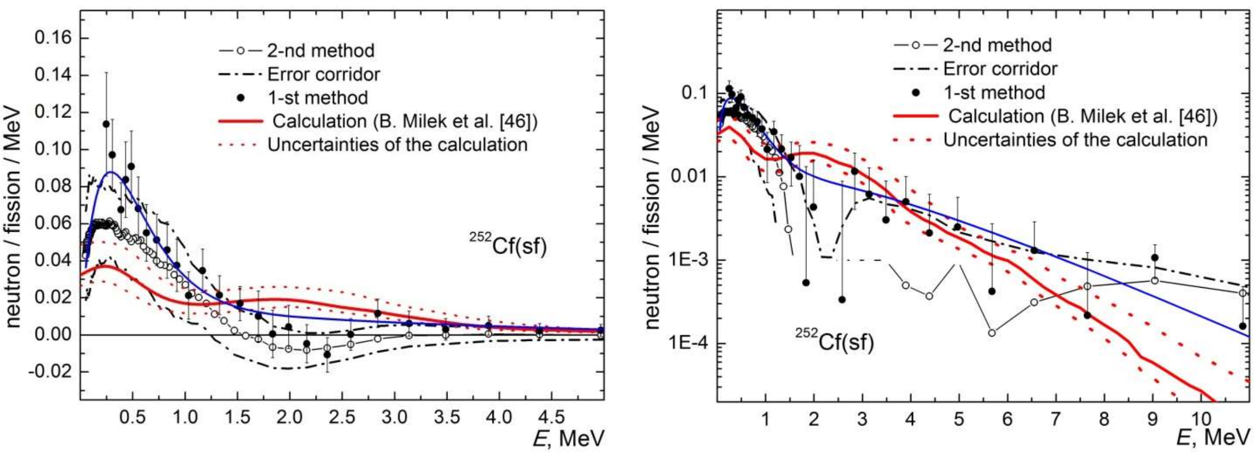

Fig. 17. *Spectrum of “scission” neutrons from the ^{252}Cf(sf) fission (left – linear scale, right - logarithmic scale). Denotations are the same as in Fig. 16. The blue curve is the result of approximation using function (14). The solid line (red) is the scission neutron yield calculated in [46]. The dotted line shows the errors of calculation [46] arising from uncertainty of the input parameters.*

Conclusion

A comparison of the measured data and our model calculations shows that the experimentally observed average total number of neutrons per fission event, the total PFN spectrum, the dependence of the PFN yield on the characteristics of the fragments, and the angular and energy distributions of PFNs are described within the model of isotropic neutron emission from fully accelerated fragments with an error less than 10%. Detailed analysis of the data shows that the model calculations must be performed using the anisotropy of prompt neutron emission in the center-of-mass system of fission fragment. It was found that in the center-of-mass system of fission fragment, the PFNs are emitted along the fission axis with a higher probability than perpendicular to it ($\psi(0°)/\psi(90°) \approx 1.07–1.09$).

The total spectra of PFNs was calculated by assuming that the PFNs emitted from fully accelerated fragments coincides with the measured spectra within the errors of the experimental data in the

neutron energy region of 0.6 to 10 MeV, and the average total number of neutrons per fission event is close to the recommended values. In the region of neutron energies below ~0.6–1 MeV, a neutron excess was observed in the experiment, relative to the model calculations.
An excess of neutrons observed at angle $\Omega = 90°$ (with respect to the direction of fragments) over the model calculations performed assuming that all PFNs are emitted from fully accelerated fragments reaches 8.5±3.2% and 7.6±2.8% for ^{239}Pu and ^{252}Cf, respectively.

The observed neutron excess cannot be explained within the model of neutron emission from fully accelerated fragments. This difference can be eliminated by assuming that there were ~2–4% of "scission" neutrons. The nature of the observed neutron excess can be determined after thorough comparison of the experimental data and the calculations using theoretical models that allow for possible PFN emission mechanisms in fission.

References

1. J. Terrell, Phys. Rev. **127**, 880 (1962).
2. H. Nifenecker, C. Signarbieux, R. Babinet, and J. Poitou, in *Proceedings of the 3rd IAEA Symposium on the Physics and Chemistry of Fission, Rochester, New York, 1973*, STI/PUB/347 (IAEA, Vienna, 1974), Vol. 2, p. 117.
3. *The Nuclear Fission Process*, Ed. by C. Wagemans (CRC, Boca Raton, FL, 1991), p. 497.
4. R. Capote, Y.-J. Chen, F.-J. Hambsch, N.V. Kornilov, J.P. Lestone, O. Litaize, B. Morillon, D. Neudecker, S. Oberstedt, T. Ohsawa, N. Otuka, V.G. Pronyaev, A. Saxena, O. Serot, O.A. Shcherbakov, N.-C. Shu, D.L. Smith, P. Talou, A. Trkov, A.C. Tudora, R. Vogt, and A.S. Vorobyev, Nucl. Data Sheets **131**, 1 (2016).
5. H.R. Bowman, S.G. Thompson, J.C.D. Milton, and W.J. Swiatecki, Phys. Rev. **126**, 2120 (1962).
6. H.R. Bowman, J.C.D Milton, et.al., Phys. Rev. **129**(**5**), 2133 (1963).
7. V.M. Piksaikin, P.P. D'yachenko, L.S. Kutsaeva, Sov. J. Nucl. Phys. **25**, 385 (1977).
8. Yu.S. Zamyatnin, D. K. Ryazanov, B. G. Basova, et al., Sov. J. Nucl. Phys. **29**, 306 (1979).
9. P. Riehs, Acta Physica Austriaca **53**, 271 (1981).
10. D. Ward, R.J. Charity, D.J. Hinde, J.R. Leigh, and J.O. Newton, Nucl. Phys. **A403**, 189 (1983).
11. E.A. Seregina and P.P. D'yachenko, Sov. J. Nucl.Phys. **42**, 845 (1985).
12. E.A. Seregina, P.P. D'yachenko, Vopr. At. Nauki Tekh., Ser.: Yad. Konstanty, No. **1**, 58 (1985).
13. H. Marten, Proc. of IAEA Consulting Meeting, INDC(NDS)-251 (Vienna, 1991), p. 23.
14. O.I. Batenkov, A.B. Blinov, M.V. Blinov, S.N. Smirnov, Proc. of IAEA Consulting Meeting, INDC(NDS)-220, Vienna (1989), p.207.
15. C. Budtz-Jorgensen and H.-H. Knitter, Nucl. Phys. A **490**, 307 (1988).
16. U. Brosa and H.H. Knitter, Z. Phys. **A343**, 39 (1992).
17. Yu. D. Kamarzhnov, V. G. Nedopekin, V. I. Rogov, and S. T. Sukhorukov, At. Energy **84**, 393 (1998).
18. A.S. Vorobyev, O.A. Shcherbakov, A.M. Gagarski, G.V. Val'ski, G.A. Petrov, EPJ Web of Conf. 8 (2010) 03004.
19. J.S. Pringle and F.D. Brooks, Phys. Rev. Letters, **35**, 1563 (1975).
20. A.M. Gagarski, I.S. Guseva, V.E. Sokolov, G.V. Val'ski, G.A. Petrov, D.O. Krinitsin, D.V. Nikolaev, T.A. Zavarukhina, V.I. Petrova, Bulletin of the Russian Academy of Sciences: Physics, **72** (**6**), 773 (2008).
21. V.E. Sokolov, G.A. Petrov, I.S. Guseva, G.V. Val'sky, A.M. Gagarski, D.V. Nikolaev, D.O. Krinitsin, V.I. Petrova, T.A. Zavarukhina, Proc. of the XVIII-th International Seminar on Interaction of Neutrons with Nuclei "Neutron Spectroscopy, Nuclear Structure, Related Topics", ISINN-18, Dubna, May 26-29, 2010, ed. A.M. Sukhovoj, JINR, Dubna, E3-2011-26 (2011), p. 108.

22. N.V. Kornilov, A.B. Kagalenko, S.V. Poupko, P.A. Androsenko, F.-J. Hambsch, Nucl. Phys. A **686**, 187 (2001).
23. J.S. Fraser and J.C. Milton, Annu. Rev. Nucl. Sci. **16**, 379 (1966).
24. A.S. Vorobyev, O.A. Shcherbakov, A.M. Gagarski, G.V. Val'ski, G.A. Petrov, Bulletin of the Russian Academy of Sciences: Physics, **82**(**10**), 1245 (2018).
25. V.E. Sokolov, G.A. Petrov, I.S. Guseva, G.V. Val'sky, A.M. Gagarski, D.V. Nikolaev, D.O. Krinitsin, V.I. Petrova, T.A. Zavarukhina, Proc. of the XVIII-th International Seminar on Interaction of Neutrons with Nuclei "Neutron Spectroscopy, Nuclear Structure, Related Topics", ISINN-18, Dubna, May 26-29, 2010, ed. A.M. Sukhovoj, JINR, Dubna, E3-2011-26 (2011), p. 108.
26. I.S. Guseva, A.M. Gagarski, V.E. Sokolov, G.A. Petrov, A.S. Vorobyev, G.V. Val'sky, T.A. Zavarukhina, Physics of Atomic Nuclei **81**(**4**), 447 (2018).
27. A.S. Vorobyev, O.A. Shcherbakov, Yu.S. Pleva, A.M. Gagarski, G.V. Val'ski, G.A. Petrov, V.I. Petrova, and T.A. Zavarukhina, Nucl. Instr. Meth. Phys. Res. A **598**, 795 (2009).
28. A. S. Vorobyev and O. A. Shcherbakov, Vopr. At. Nauki Tekh., Ser.: Yad. Konstanty, Nos. 1–2, 37 (2011–2012).
29. A.S. Vorobyev and O. A. Shcherbakov, Vopr. At. Nauki Tekh., Ser.: Yad. Reac. Konstanty, No. 2, 52 (2016).
30. W. Mannhart, Proc. of IAEA Consulting Meeting, INDC(NDS)-220, Vienna (1989), p. 305.
31. J. Terrell, Phys. Rev. **113**, 527 (1959).
32. D.G. Madland and J.R. Nix, Nucl. Sci. Eng. **81**, 213 (1982).
33. N.V. Kornilov, A.B. Kagalenko and F.-J. Hambsch, Phys. At. Nucl. **64**(8), 1373 (2001).
34. J. Terrell, Phys. Rev. **127**, 880 (1962).
35. K. Skarsvag, Physica Scripta 7, 160 (1973).
36. V.E. Bunakov, I. S. Guseva, S.G. Kadmenskii, and G. A. Petrov, Izv. Akad. Nauk, Ser. Fiz. **70**, 1618 (2006).
37. J. Randrup, R. Vogt, Physics Procedia **64**, 19 (2015).
38. J. C. D. Milton and J. S. Fraser, Phys. Rev. **111**, 877 (1958).
39. T. Haninger, F.-J. Hartmann, P. Hofmann, Y.S. Kim, M.S. Lotfranaei, T. von Egidy, H. Marten, and A. Ruben, Nucl. Phys. A **572**, 294 (1994).
40. A.S. Vorobyev, O.A. Shcherbakov, A.M. Gagarski, G.A. Petrov, G.V. Val'ski, Journal of Experimental and Theoretical Physics 125(4), 619 (2017).
41. A.S. Vorobyev, O.A. Shcherbakov, A.M. Gagarski, G.A. Petrov, G. V. Val'ski, T.E. Kuz'mina, Journal of Experimental and Theoretical Physics 127(4), 659 (2018).
42. A. Göök, F.-J. Hambsch, and M. Vadali, Phys. Rev. C **90**, 064611 (2014)
43. A.D.G. Madland and A. C. Kahler, Nucl. Phys. A **957**, 289 (2017).
44. M. Rizea, N. Carjan, and T. Wada, Physics Procedia **47**, 27 (2013).
45. T. Wada, T. Asano, and N. Carjan, Physics Procedia **64**, 34 (2015).
46. B. Milek, R. Reif, and J. Révai, Phys. Rev. C **37**, 1077 (1988).

Appendix 1

The main characteristic of the $^{239}Pu(n_{th},f)$ fission fragments

Ref.	Method	$\langle m^*_L \rangle$	$\langle V^*_L \rangle$	$\langle V^*_H \rangle$	$\langle E^*_L \rangle$	$\langle TKE \rangle$
[1]	2v-2E, 2SSBD	100.9	1.41	1.02	103.5 ± 1.0	178.9 ± 1.2
[2]	2v	100.23	1.39	1.005	101.5 ± 1.0	174.4 ± 1.7
[3]	2v, 2SSBD	100.85	1.4063	1.0192	103.02 ± 0.3	177.88 ± 0.40
[4]	2E, 2SSBD	100.34			103.2 ± 1.0	177.7 ± 1.8
[5]	2E, 2SSBD	100.3			103.29 ± 0.01	177.65 ± 0.01
[6]	2E, 2SSBD	100.6			104.0 ± 1.5	179.3 ± 2.0
[7]	E-v, SSBD, PPAC	100.3			102.0 ± 1.0	176.2 ± 1.4
[8]	2E, 2SSBD	100.57			103.35 ± 0.3	177.9 ± 0.4
Average		100.5 ± 0.1			103.1 ± 0.5	177.5 ± 0.7
Recommended-V.G. Vorobyev, V.D. Kuzminov, VANT Ser. Nucl. Const. 1985, N2, p. 27						178.6 ± 0.9
Recommended (In book "The Nuclear fission process" Boca Raton, Florida, 1991, p. 323)						177.9 ± 0.5

[1]. K. Nishio, Y. Nakagome, I. Kanno and I. Kimura, "Measurement of fragment mass dependent kinetic energy and neutron multiplicity for thermal neutron induced fission of plutonium-239"// *J. Nucl. Sci. Tech.*, 32, 404-414 (1995).

[2]. J.C.D. Milton, J.S. Fraser, "Time-of-Flight fission studies on ^{233}U, ^{235}U and ^{239}Pu" // *Can. J. Phys.*, 40, 1626 (1962).

[3]. P. Geltenbort, F. Gonnenwein and A. Oed, "Precision measurements of mean kinetic energy release in thermal-neutron-induced fission of ^{233}U, ^{235}U and ^{239}Pu" // *Radiat. Effects*, 93, 57 (1986).

[4]. J.N. Neilier, F.J. Walter and H.W. Schmitt, "Fission-fragment energy-correlation measurements for the thermal-neutron fission of ^{239}Pu and ^{241}Pu" // *Phys. Rev.*, 149, 894-905 (1966).

[5]. C. Wagemans, E. Allaert, A. Deruytter, R. Barthelemy, P. Schillebeeckx, "Comparision of the energy and mass characteristics of the $^{239}Pu(n_{th},f)$ and the $^{240}Pu(sf)$ fragments" // *Phys. Rev.*, C30, 218-233 (1984).

[6]. M.J. Bennett and W.E. Stein, "Kinetic energy of fragments from seven fission reaction at low excitation energies" // *Phys. Rev.,* 156, 1277-1282 (1967).

[7]. C. Tsuchiya, Y. Nakagome, H. Yamana, *et.al.*, "Simultaneous measurement of prompt neutrons and fission fragments for $^{239}Pu(n_{th},f)$" // *J. Nucl. Sci. Tech.*, 37, 941-948 (2000).

[8]. M. Asghar, F. Caitucoli, P. Perrin and C. Wagemans, "Fission fragment energy correlation measurements for the thermal neutron fission of ^{239}Pu and ^{235}U" // *Nucl. Phys.*, A311, 205-218 (1978).

Appendix 2

The main characteristic of the $^{252}Cf(sf)$ fission fragments

Ref.	Method	$<m^*_L>$	$<V^*_L>$	$<V^*_H>$	$<E^*_L>$	<TKE>
[1]	2v	108.39	1.375	1.036	105.7 ± 1.1	185.7 ± 1.8
[2]	2v	108.25	1.370	1.034	105.7 ± 1.0	185.3 ± 1.7
[3]	2v	108.46	1.370	1.036	105.1 ± 1.0	184.9 ± 2.0
[4]	2E, 2SSBD	108.55			106.2 ± 0.7	186.5 ± 1.2
[5]	2E, 2SSBD	109.0			106.3 ± 0.7	187.3 ± 1.7
[6]	2E, 2SSBD	108.2			105.1 ± 1.5	184.3 ± 2.0
[7]	2E, 2SSBD	108.55			105.9 ± 0.7	186.2 ± 1.2
[8]	2E, 2SSBD	108.6			105.5 ± 0.6	185.8 ± 1.0
Average		108.5 ± 0.1			105.5 ± 0.6	185.3 ± 0.9
Recommended-V.G. Vorobyev, V.D. Kuzminov, VANT Ser. Nucl. Const. 1985, N2, p. 27						186.3 ± 1.0
Recommended (In book "The Nuclear fission process" Boca Raton, Florida, 1991, p. 323)						184.1 ± 1.3

[1]. S.L. Whetstone, Jr. "Coincident time-of-flight measurements of the velocities of ^{252}Cf fission fragments" // *Phys. Rev.*, 131, 1232-1243 (1963).

[2]. J.S. Fraser, J.C.D. Milton, H.R. Bowman and S.G. Thompson "" // *Can. J. Phys.*, 41, 2080 (1963).

[3]. Yu.A. Barashkov et al, "TOF measurements of the corresponding fission fragments in spontaneous fission of Cm-244 and Cf-252" // *Yad. Fiz.* 13(6), 1162 (1971) (in Russian).

[4]. H.W. Schmitt, J.N. Neilier and F.J. Walter, "Fragment energy correlation measurements for ^{252}Cf spontaneous fission and ^{235}U thermal-neutron fission" // *Phys. Rev.*, 141, 1146-1160 (1966).

[5]. A. Gavron and Z. Fraenkel "Neutron correlations in spontaneous fission of ^{252}Cf" // *Phys. Rev.*, C9, 632-645 (1974).

[6]. M.J. Bennett and W.E. Stein, "Kinetic energy of fragments from seven fission reaction at low excitation energies" // *Phys. Rev.,* 156, 1277-1282 (1967).

[7]. R. Schmidt and H. Henschel "Comparison of the spontaneous fission of ^{244}Cm and ^{252}Cf: (I). Fragment masses and kinetic energies" // *Nucl. Phys.*, A395, 15-28 (1983).

[8]. G. Barreau, A. Sicre, F. Caitucoli, M. Asghar, T.P. Doan, B. Leroux, G. Martinez and T. Benfoughal, "Fission-fragment energy correlation measurements for $^{252}Cf(sf)$ and structure in far-out asymmetric fission" // *Nucl. Phys.*, A432, 411-420 (1985).

Nuclear Data Section
International Atomic Energy Agency
Vienna International Centre, P.O. Box 100
A-1400 Vienna, Austria

E-mail: nds.contact-point@iaea.org
Telephone: (43-1) 2600 21725
Web: http://nds.iaea.org